Myocardial T_1 Mapping: Application to Patients With Acute and Chronic Myocardial Infarction

Daniel R. Messroghli,[1,2*] Kevin Walters,[3] Sven Plein,[1] Patrick Sparrow,[1] Matthias G. Friedrich,[4,5] John P. Ridgway,[6] and Mohan U. Sivananthan[1]

T_1 maps obtained with modified Look-Locker inversion recovery (MOLLI) can be used to measure myocardial T_1. We aimed to evaluate the potential of MOLLI T_1 mapping for the assessment of acute and chronic myocardial infarction (MI). A total of 24 patients with a first MI underwent MRI within 8 days and after 6 months. T_1 mapping was performed at baseline and at selected intervals between 2–20 min following administration of gadopentetate dimeglumine (Gd-DTPA). Delayed-enhancement (DE) imaging served as the reference standard for delineation of the infarct zone. On T_1 maps the myocardial T_1 relaxation time was assessed in hyperenhanced areas, hypoenhanced infarct cores, and remote myocardium. The planimetric size of myocardial areas with standardized T_1 threshold values was measured. Acute and chronic MI exhibited different T_1 changes. Precontrast threshold T_1 maps detected segmental abnormalities caused by acute MI with 96% sensitivity and 91% specificity. Agreement between measurements of infarct size from T_1 mapping and DE imaging was higher in chronic than in acute infarcts. Precontrast T_1 maps enable the detection of acute MI. Acute and chronic MI show different patterns of T_1 changes. Standardized T_1 thresholds provide the potential to dichotomously identify areas of infarction. Magn Reson Med 58: 34–40, 2007. © 2007 Wiley-Liss, Inc.

Key words: myocardial infarction; magnetic resonance imaging; T_1 mapping; relaxation time; infarct area

In present imaging techniques for in vivo infarct sizing, such as cardiac magnetic resonance (CMR) and single-photon emission computed tomography (SPECT), the viewing window (i.e., the range of gray/color values to be selected for viewing) is determined arbitrarily before reporting, and thus requires a subjective preassessment of the images.

In CMR the delayed-enhancement (DE) method produces high contrast between infarcted and noninfarcted myocardium (bright = dead). The observable high contrast is reliant upon the imaging strategy employed. A preparatory inversion-recovery pulse in a T_1-weighted gradient-echo sequence nulls signal from noninfarcted myocardium, while infarcted myocardium, which retains a higher concentration of a gadolinium (Gd)-based extracellular contrast agent, returns higher signal due to its reduced spin-lattice relaxation time (T_1 time) (1). The contrast between infarcted and noninfarcted areas on the resulting images is therefore enhanced over and above the underlying physical differences in T_1 relaxation properties between these areas. The apparent degree of enhancement is dependent on the effectiveness of the nulling process, which is a function of the inversion time (TI) selected for the preparation pulse. Incomplete nulling will cause reduced contrast and create significant variation in the signal of remote myocardium, which is used as the reference to determine the threshold between infarcted and noninfarcted myocardium (2). The choice of TI therefore ultimately influences the infarct size as measured with DE techniques.

T_1-mapping CMR techniques circumvent the influences of windowing and variations in signal enhancement by directly measuring the underlying T_1 relaxation times of the different areas of the myocardium. At a given magnetic field strength, each tissue has a normal range for spin-lattice T_1 relaxation time (3,4), much like the normal ranges of tissue X-ray attenuation in computed tomography (CT) measured in Hounsfield units. Thus by encoding CMR images by actual T_1 relaxation times, one could prescribe standardized cutoffs between "normal" and "affected" myocardium to eliminate observer-input in delineation of diseased myocardium.

The modified Look-Locker inversion recovery (MOLLI) technique was recently proposed as a means of creating high-resolution single-slice maps of myocardial T_1 relaxation times (5), and normal values for human myocardium have been established using this technique (6). We hypothesized that thresholds derived from these normal values, when applied to T_1 maps of patients with myocardial infarction (MI), could accurately delineate areas of MI.

MATERIALS AND METHODS

Patients

Twenty-four patients (20 males and four females, mean age = 57.8 ± 12.6 years) from The Leeds General Infirmary and St. James's University Hospital, Leeds, UK, who presented with acute MI were enrolled and underwent CMR imaging 4.5 ± 1.7 days (range = 2–8 days) after onset of symptoms and again after 6 months (196 ± 40 days, range = 133–280 days) at the BHF Cardiac MRI Unit, Leeds. Patients were eligible for inclusion if they had 1) typical chest pain for >30 min; 2) infarct-related changes on a 12-lead electrocardiogram (ECG); 3) elevated troponin

[1]BHF Cardiac MRI Unit, Leeds General Infirmary, Leeds, UK.
[2]Cardiac MRI Unit, Franz Volhard Klinik, Charité/Humboldt Universität, Berlin, Germany.
[3]Division of Genomic Medicine, University of Sheffield, Sheffield, UK.
[4]Department of Cardiac Sciences, Stephenson CMR Centre, University of Calgary, Calgary, Canada.
[5]Department of Radiology, Stephenson CMR Centre, University of Calgary, Calgary, Canada.
[6]Department of Medical Physics, Leeds General Infirmary, Leeds, UK.

Grant sponsor: European Commission.

*Correspondence to: Dr. Daniel Messroghli, Arbeitsgruppe Kardiale MRT, Franz Volhard Klinik, Charité Campus Buch, Wiltbergstrasse 50, 13125 Berlin, Germany. E-mail: daniel.messroghli@charite.de

Received 5 December 2006; revised 20 February 2007; accepted 27 March 2007.
DOI 10.1002/mrm.21272
Published online in Wiley InterScience (www.interscience.wiley.com).

levels, (d) peak creatine kinase levels >300 IU/l; 4) no previous history of MI, coronary intervention, or heart disease of any other etiology; and 5) no contraindication to CMR (e.g., claustrophobia or noncompatible metallic implants). The study complied with the Declaration of Helsinki and was approved by the local ethics committees, and all subjects gave written informed consent.

T_1 Mapping Technique

We applied a previously described MOLLI pulse sequence that acquires a set of 11 source images of the patient within one breath-hold (16–20 s), allowing the reconstruction of one parametric T_1 map (5). The source images are all identical (i.e., with the same voxel size, image position, and phase of the cardiac cycle) except for different effective TIs. This is achieved by performing three different ECG-triggered inversion recovery-prepared experiments (TI = 100, 200, and 350 ms), each followed by several single-shot image acquisitions (<200 ms) at end-diastole of consecutive heartbeats. A balanced steady-state free precession (bSSFP) sequence was used for readout (TR = 3.9 ms, TE = 1.95 ms, flip angle = 50°, sensitivity-encoding (SENSE) factor = 2, field of view (FOV) = 380 × 342 mm, matrix = 240 × 151, slice thickness = 8 mm).

Imaging Protocol

All studies were performed on a 1.5T MR system (Gyroscan Intera CV with Master gradients, 30 mT/m, 150 T/m/s; Philips, Best, The Netherlands). An identical T_1-mapping protocol was carried out on both initial and follow-up scans as previously described for healthy volunteers (6).

After the acquisition of a SENSE reference scan, precontrast MOLLI sequences were performed at the mid-cavity, basal, and apical short-axis levels, which were defined as the middle three of five short-axis slices positioned between the mitral annulus and the left ventricular tip on systolic long-axis cine images (7). Following this, gadopentetate dimeglumine (Gd-DTPA; Magnevist; Schering AG, Berlin, Germany) was administered intravenously at a dose of 0.15 mmol/kg of body weight using an automated injection pump (Spectris Solaris; Medrad Inc., Indianola, PA, USA). The dose of the contrast agent was divided to allow integration of this protocol into existing perfusion protocols. After the first injection (0.05 mmol/kg, rate 5 ml/s, 10-ml saline flush), there was a 60-s delay (as required for first-pass perfusion imaging) before the second injection (0.1 mmol/kg) was administered. MOLLI was performed consecutively at all three short-axis levels at 2, 4, 6, 8, 10, 15, and 20 min after the second injection.

In order to optimize the choice of TI for DE imaging, the TI that achieved the best nulling of the myocardium was determined from four test images with increasing TIs (240–300 ms in steps of 20 ms) between MOLLI acquisitions at 10 and 15 min. Using this TI, breath-hold DE imaging was subsequently performed at the same three short-axis levels using the same image geometry as for the MOLLI sequences (inversion recovery-prepared gradient-echo, TR = 4.7 ms, TE = 2.0 ms, flip angle = 15°, FOV = 380 × 342 mm, matrix = 240 × 151, slice thickness = 8 mm).

Reconstruction of T_1 Maps

T_1 maps were constructed offline using a customized software program written in Interactive Data Language (IDL; RSI International, Boulder, CO, USA). The position of the source images was initially manually adjusted to correct for potential misregistration caused by translational displacement in case of poor breath-holding. A three-parameter curve fit of the MOLLI source images was then performed, with automatic calculation of T_1 values for each pixel. A T_1 parametric map was subsequently generated and saved as a DICOM image for further analysis (5).

Image Analysis

All analysis of DE images and T_1 maps was performed with a commercial software package for the evaluation of CMR data (Mass 5.0; Medis, Leiden, The Netherlands). The evaluation was performed in three steps as described below:

DE Analysis

In every patient the short-axis level (basal, mid-cavity, or apical) with the largest extension of hyperenhancement on DE images was selected for all infarct analysis. The epi- and endocardial contours of the left ventricle were drawn on DE images at the selected short-axis level, and the myocardial surface area was noted. The circumference of the myocardium was divided into six segments. A region of interest (ROI) was placed in the myocardial segment directly opposite to the area of hyperenhancement ("remote area"). Using the mean and SD values of the signal intensities (SIs) within this ROI, the image was then viewed in black/white contrast using a 2-SD SI threshold as established in experimental validation studies of DE imaging (8,9):

$$\text{threshold}_{\text{DE}} = \text{mean\_SI}_{\text{remote\_area}} + 2 \times (\text{SD\_SI}_{\text{remote\_area}})$$

The resulting bright area within the left ventricular myocardium was outlined with a ROI ("hyperenhanced area"). The planimetric size of the hyperenhanced area was noted and expressed as a percentage of the myocardial surface area. If subendocardial dark areas of ≥4 contiguous pixels were present in the center of the hyperenhanced area, they were outlined by another ROI ("hypoenhanced core").

Analysis of T_1 in Different Areas of the Myocardium

The ROIs from the DE analysis were copied onto the full set of T_1 maps (1 × precontrast, 7 × postcontrast) at the selected short-axis level and manually corrected for any evident misregistration. T_1 values were noted for remote area, hyperenhanced area, and hypoenhanced core (if present) for all time points. In a previous study, the heart-rate (HR) dependency of MOLLI T_1 measurements was observed in T_1 values > 600 ms as present in myocardium pre- but not postcontrast. Therefore, precontrast T_1 values were corrected for HR using

$$T_{1\text{corrected}} = T_{1\text{raw}} - (2.7 \times (\text{HR} - 70))$$

as empirically derived from a previous study of healthy volunteers (6).

T_1 Thresholds: Infarct Sizing

At the start of this analysis, all drawn ROIs were removed from the T_1 maps, with only the endo- and epicardial left ventricular contours remaining. Precontrast T_1 maps were viewed in black/white contrast with a threshold set at the mean + 3 SD of the normal myocardial T_1 values previously established in healthy volunteers (2-SD thresholds were also tested, but yielded inferior diagnostic accuracy; data not shown). In order to adjust for the precontrast HR dependency cited above, the precontrast threshold value was corrected for HR for a given patient using the following equation (6):

$$\text{threshold}_{\text{raw\_maps}} = \text{threshold}_{\text{normal}} + (2.7 \times (\text{HR} - 70))$$

Bright areas were then outlined with an ROI ("infarct-area/precontrast"). The planimetric size of these ROIs was noted and expressed as a percentage of the myocardial surface area. In postcontrast T_1 maps, black/white contrast was created by setting thresholds of mean–3 SD using the normal values for the given time points. Since HR correction in MOLLI T_1 maps is only required for T_1 values $>$ 800 ms (as present in precontrast myocardium), no further adjustments were necessary for the postcontrast T_1 maps. The planimetric size of ROIs defining black areas of the myocardium ("infarct-area/postcontrast") was noted (subendocardial white areas corresponding to hypoenhanced cores on DE images were included in the ROIs).

T_1 Thresholds: Segmental Infarct Detection

Myocardial defects were noted for DE images (areas of hyperenhancement), precontrast 3-SD threshold T_1 maps (bright areas), and postcontrast 3-SD threshold T_1 maps (black areas). Myocardial segments were considered as "positive" (affected by the infarction) if there was a defect of ≥4 contiguous pixels linked to the endocardial border within the segment.

Statistical Analysis

Paired Student's *t*-tests were used to compare continuous data within patients. Subgroup analysis was performed using independent-sample *t*-tests. Bland-Altman analysis was performed to assess agreement of infarct size measurements. All statistical analysis was performed using a statistical software package (Analyze-it 2002; Analyze-it Software Ltd., Leeds, UK). All values are given as the mean ± SD. A *P*-value < 0.05 was deemed significant.

RESULTS

Patient Population

Infarct localization on ECG was anterior in 11 cases, inferior in 12, and posterolateral in one. Fourteen patients (58.3%) received primary thrombolysis therapy, and 11 (45.8%) underwent percutaneous coronary intervention of the culprit lesion before ($N = 3$) or after ($N = 8$) the first CMR scan. Peak creatine kinase was 2177 ± 1669 IU/l (range = 348–6200 IU/l).

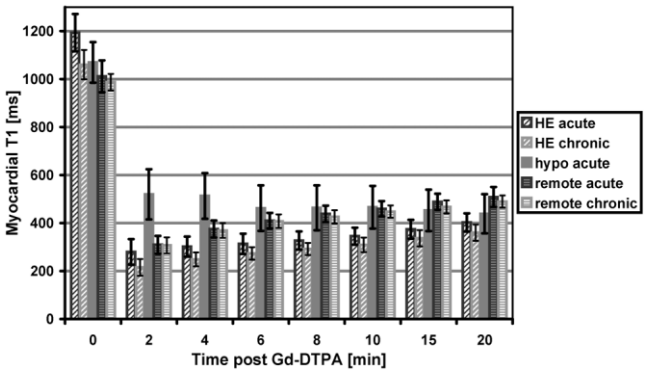

FIG. 1. Mean myocardial T_1 relaxation times of acute and chronic studies in hyperenhanced (HE) areas ($N = 24$), remote areas ($N = 24$), and hypoenhanced cores (acute only, $N = 14$), pre- (minute 0) and postadministration of Gd-DTPA (0.15 mmol/kg). Error bars represent the standard deviation (SD).

DE Analysis

The short-axis slice selected for evaluation was mid-cavity in 19 cases and basal in five. The planimetric size of the infarcted area (expressed as a percentage of the left ventricular myocardium of the same slice) on DE images was larger in the acute than in the chronic stage (33.0 ± 15.9 vs. 30.4 ± 13.9%, $P < 0.05$). Significant hypoenhanced cores were present in 14 patients (58.3%) in the acute stage, but there were none in the chronic stage. Patients who presented with hypoenhanced cores had higher peak creatine kinase levels than those who did not (2780 ± 1847 vs. 1333 ± 910 U/l, $P < 0.033$).

Analysis of T_1 in Different Areas of the Myocardium

A total of 192 maps (eight per patient) were analyzed. Six T_1 maps (3.1%) were discarded due to ECG trigger artifacts during image acquisition, leaving 186 available for evaluation.

Figure 1 illustrates the course of T_1 relaxation times in remote areas, hyperenhanced areas, and hypoenhanced cores. In chronic MI the precontrast T_1 relaxation time of hyperenhanced areas was higher than the T_1 of remote areas (1060 ± 61 vs. 987 ± 34 ms, $P < 0.0001$). In acute MI the precontrast T_1 value of hyperenhanced areas was even higher than in chronic MI (1197 ± 76 vs. 1060 ± 61 ms, $P < 0.0001$), while remote T_1 values were not significantly different from chronic remote areas (1011 ± 66 vs. 987 ± 34 ms, $P = 0.13$).

The administration of contrast agent led to shorter T_1 times in hyperenhanced areas as compared to remote areas at all time points in both acute and chronic studies (2–20 min, $P < 0.007$). At follow-up, postcontrast T_1 values of hyperenhanced areas were lower compared to the acute studies (all $P < 0.0015$). However, contrast-induced T_1 shortening in hyperenhanced areas, as expressed by the

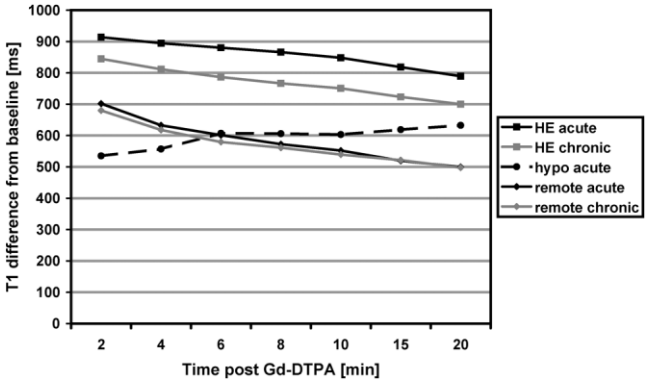

FIG. 2. Mean contrast-induced T_1 shortening in HE areas, remote areas, and hypoenhanced cores as expressed by the difference between baseline and postcontrast T_1 at different time points.

difference between baseline and postcontrast T_1s, was significantly more pronounced in the acute than in the chronic studies at all time points ($P < 0.011$; Fig. 2).

Precontrast, the T_1 values of hypoenhanced cores showed a trend toward higher values compared to those of remote areas (1069 ± 85 vs. 1022 ± 77 ms, $P = 0.085$), but were lower than those of surrounding hyperenhanced infarct areas (1069 ± 85 vs. 1175 ± 86 ms, $P < 0.0006$). At 2 min postcontrast the T_1 values of hyperenhanced and remote areas had already dropped to their minimum values (23.4% and 30.6% from precontrast, respectively) and then subsequently started to recover. The T_1 values in hypoenhanced cores only dropped to 48.6% at 2 min, and continued to fall over the course of 20 min to 41.0% of their precontrast T_1 value.

T_1 Threshold Analysis

Table 1 gives the threshold values (derived from a previous volunteer study (6)) that were used for analysis. Figure 3 shows a set of DE images and T_1 maps from acute and chronic studies of a 41-year-old patient with anteroseptal MI using full grayscale and threshold viewing.

Figure 4 shows the sensitivities and specificities of 3-SD threshold T_1 maps for identifying segments affected by MI as compared to DE imaging as the reference standard. Of a total of 144 myocardial segments, 52 and 59 were rated "positive" on acute and chronic DE images, respectively. In the acute studies, sensitivities and specificities were high both pre- and postcontrast. In the chronic studies, sensitivities and specificities were limited precontrast but were very high for postcontrast T_1 maps.

Table 1
Normal Myocardial T_1 Relaxation Times and Threshold Values

Time point	Mean ± SD (ms)	3-SD threshold (ms)
Precontrast	982 ± 46	1120
2 min p.c.	344 ± 35	239
4 min p.c.	402 ± 32	306
6 min p.c.	436 ± 31	343
8 min p.c.	455 ± 29	368
10 min p.c.	470 ± 26	392
15 min p.c.	494 ± 23	425
20 min p.c.	510 ± 23	441

SD = standard deviation, p.c. = postcontrast.

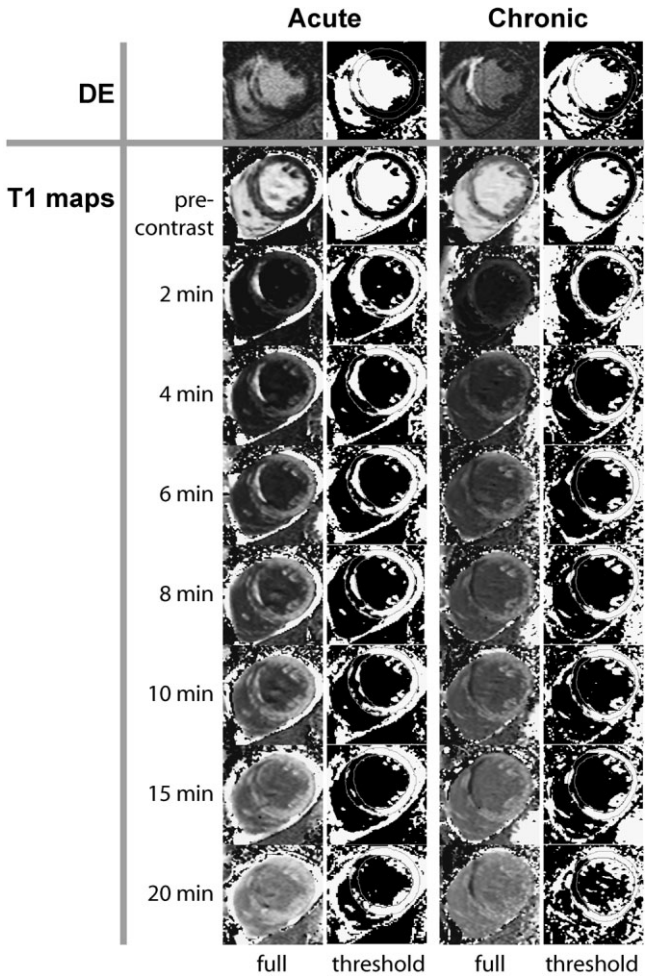

FIG. 3. Midcavity short-axis DE images and T_1 maps acquired 5 days ("acute") and 280 days ("chronic") after anteroseptal ST-elevation MI in a 41-year-old male. Images are shown with both full grayscale ("full") and black/white contrast ("threshold") using thresholds of 2 SDs above the remote SI (DE) or 3 SDs beyond the standardized normal T_1 relaxation time (T_1 maps). The patient received primary thrombolytic therapy but showed no immediate resolution of ST segments on ECG (peak creatine kinase = 4891 U/l). In the acute stage, there is a large hypoenhanced core (as a sign of no-reflow) that is black on the DE image and white on the T_1 maps during the first minutes after the administration of contrast agent.

In the acute stage, T_1 thresholds identified the infarct area as localized by DE imaging in all cases precontrast and in all T_1 maps after contrast agent, but for only four cases at 2 min. In the chronic stage the infarct areas were always delineated, except for five cases (20.8%) precontrast and one case (4.2%) at 2 min postcontrast.

Figure 5 shows the mean differences between the percentages of infarcted myocardium as assessed by T_1 relaxation time threshold analysis and DE analysis. The Bland-Altman analysis of the 20-min data is given in Fig. 6, illustrating the agreement between DE and T_1 threshold results in more detail.

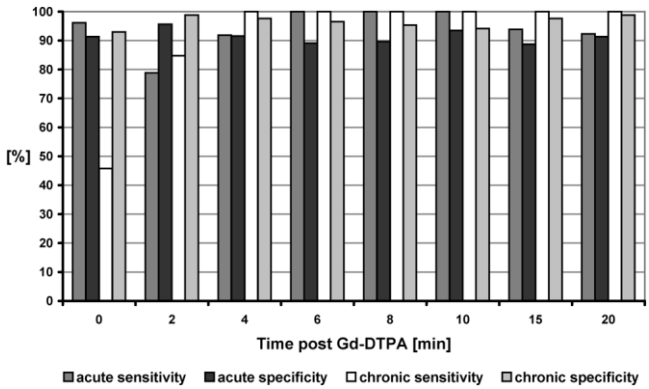

FIG. 4. Sensitivities and specificities of T_1-map threshold viewing at different time points to identify segments of MI in the acute and chronic stages as compared to standard DE imaging. Minute 0 = precontrast.

DISCUSSION

This study confirms the hypothesis that threshold T_1 relaxation time values derived from normal myocardium can be used to differentiate infarcted from noninfarcted myocardium in an observer-independent fashion.

We tested whether T_1 thresholds could be used to dichotomously identify areas of MI. With the T_1-threshold approach, infarcted segments could be identified with very high sensitivity and specificity. Interestingly, precontrast 3-SD threshold T_1 mapping detected segmental defects caused by acute MI with 96% sensitivity and 91% specificity, respectively. Postcontrast, the sensitivities and specificities for detecting infarcted segments were higher in chronic than in acute studies. These findings are explained by the results from our analysis of T_1 relaxation times in the different areas of the myocardium pre- and postcontrast, which in this study were investigated for the first time serially in the same cohort of patients in the acute and chronic stages of MI. We found that the precontrast T_1 relaxation time was higher in infarcted than in remote areas, with highest values in the acute stage. This is in good agreement with a serial animal study performed on a low-field MR system, in which T_1 relaxation times of infarcted (reperfused and non-reperfused) myocardium after 3 weeks were still higher than those of remote areas, but lower compared to infarcted areas at 5 days (10). As for nonquantitative T_2-weighted techniques, the underlying mechanism of precontrast signal changes in acute infarcts is likely to be myocardial edema, which causes prolongation of both T_1 and T_2 times (11,12). Post administration of contrast medium, T_1 relaxation time of infarcted myocardium was shorter at the chronic stage than at the acute stage. This explains why in clinical CMR, DE imaging in chronic infarcts tends to result in brighter hyperenhancement than in acute infarcts. However, contrast-induced T_1 shortening, as expressed by the difference between pre- and postcontrast T_1s, was more pronounced in acutely infarcted areas, where the baseline T_1 was much higher. This is in agreement with animal studies that showed that the increase in the volume of distribution for extracellular contrast agents caused by the loss of cell membrane integrity in acute necrosis is higher than that caused by the expansion of extracellular space in chronic scarification (13–15).

The T_1-threshold approach was also used to measure the fraction of infarcted myocardium within the imaging plane. Infarct size was overestimated beyond 4 min postcontrast by a mean of $<7\%$ in acute and $<5\%$ in chronic stages, respectively (Fig. 5). From a technical point of view, possible explanations for overestimation of infarct size are an insufficient contrast-to-noise ratio (CNR) of the source images, and partial-volume effects due to misregistration during the "curve-fitting" process. Future developments should therefore focus on further enhancing spatial resolution (e.g., by the use of shorter TRs), and on automated image registration, which could make use of statistical methods to optimize the quality of the T_1 fitting curves. However, technical considerations alone do not explain why variation in the postcontrast infarct size measurements (as illustrated by the Bland-Altman bias plots, Fig. 6) was more pronounced in acute than in chronic studies. This additional variation may be caused by the more heterogeneous nature of the border of acute myocardial necrosis as compared to that of chronic myocardial scarring, where a zone of "intermediate" enhancement was recently observed in DE imaging (16). These intermediate signal changes may not always reach threshold levels for both methods. The use of a recently proposed semiautomatic software technique based on region-growing algorithms might have reduced variations in the DE results, but this technology was not available for our study (17).

The MOLLI technique used in this study provides single-breath-hold T_1 mapping with high-precision, pixel-by-pixel measurements of T_1 relaxation times (5,6). The spatial resolution of our T_1 maps was sufficient to determine T_1 relaxation times in hypoenhanced cores, which have been shown to have a high prognostic value (18) and have been used as a target parameter for therapeutic interventions (19). Our results show that the wash-in of contrast medium in these areas is extremely prolonged, with T_1 relaxation times continuing to decrease at 20 min post administration of contrast. This finding supports the hypothesis that hypoenhanced cores represent areas of microvascular obstruction in which perfusion is abolished whether or not macrovascular blood flow is reestablished.

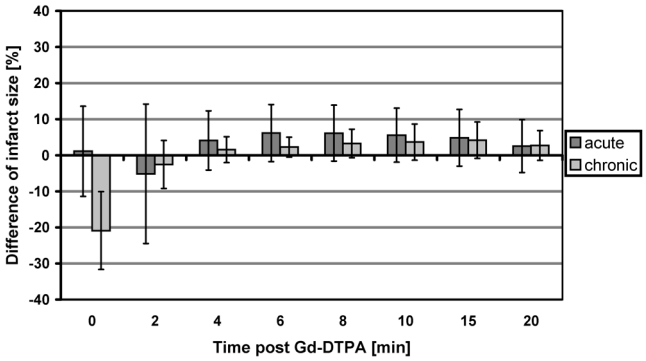

FIG. 5. Difference of percentage infarct size between T_1-threshold analysis at different time points and DE analysis, in acute and chronic stages. Error bars represent the SD; 0 min = preadministration of Gd-DTPA.

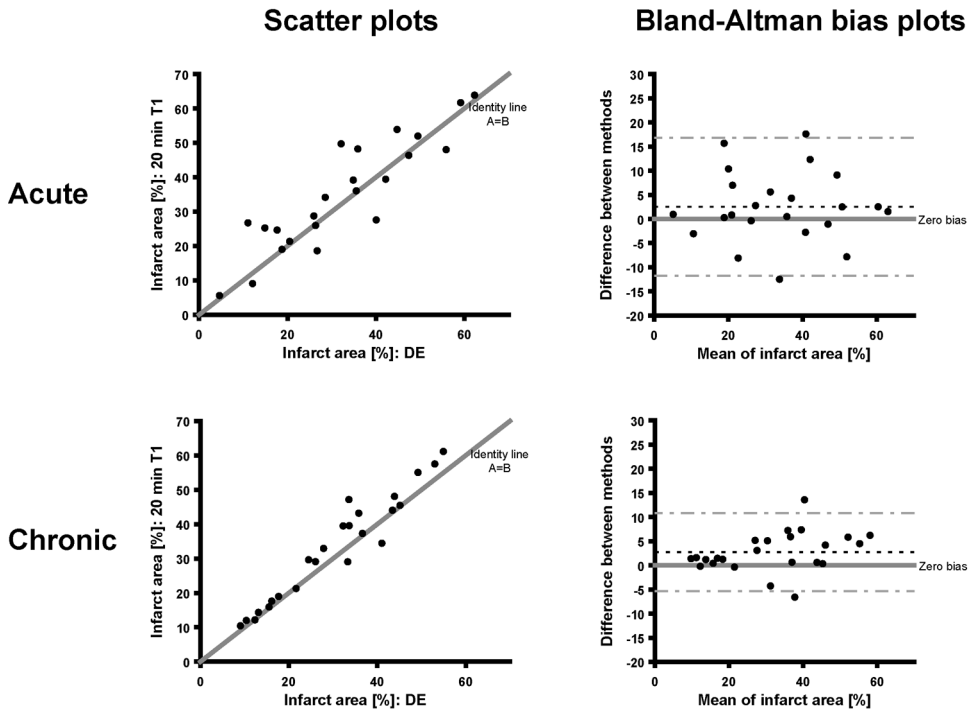

FIG. 6. Scatter plots and Bland-Altman bias analysis of the T_1-threshold approach at 20 min postcontrast compared to DE imaging, in acute and chronic stages. The mean difference (bias) was 2.52% (95% CI: −0.64 to 5.68) in acute and 2.72% (95% CI: 0.98–4.46) in chronic studies, respectively. Dotted line = bias (mean difference between methods); dashed lines = 95% limits of agreement.

Clinical Implications

Our results show that T_1 thresholds can be used to identify the area of infarction in T_1 maps of patients with MI, without the need to adjust the TI during the scanning. While DE imaging is a simple and well-established technique, and therefore the tool of choice for visualizing MI at present, the access to quantitative and more detailed information on myocardial signal behavior provided by T_1 mapping may add valuable insights, e.g., into the acuteness of MI. Future technical advances may help overcome overestimation of infarct size and make this technique suitable for semiautomatic measurements of infarct size in a clinical setting. Follow-up studies assessing the recovery of left ventricular function post revascularization will be necessary to determine the sensitivity and specificity of this technique for detecting myocardial viability.

Quantitative T_1 measurements were recently used to characterize T_1 changes in patients with cardiac amyloidosis (20). The ability to differentiate "normal" from "abnormal" myocardial SIs also suggests an important diagnostic potential for threshold-based T_1 analysis in patients with other myocardial diseases, such as viral myocarditis. Since inflammatory processes frequently are diffuse rather than discrete processes, conventional techniques, which rely on the comparison of "remote" areas with "affected" areas, may not be favorable to assess these global effects adequately. Therefore, threshold-based T_1 mapping could be a suitable tool to directly identify inflamed myocardium without the need for comparison with nonaffected areas of the myocardium (21) or skeletal muscle (22).

Limitations

Not all of our patients underwent X-ray coronary angiography, and while 14 (58%) received primary thrombolytic therapy, only five (21%) showed clinical signs of reperfusion (e.g., pain relief or resolution of ST segments on ECG). Therefore, it was not possible to compare findings between patients with reperfused vs. non-reperfused MI. The dose of the contrast agent used in this study was 0.15 mmol/kg body weight. Previous animal studies comparing DE and histologic infarct size were performed with doses as high as 0.3 mmol/kg (8); however, doses of 0.1–0.15 mmol/kg are recommended for clinical MRI (2). The T_1 relaxation time thresholds used were specifically derived for the contrast regimen of this study. Therefore, our results do not allow any conclusion to be drawn regarding the potential of T_1 thresholds with other doses of contrast medium.

CONCLUSIONS

Precontrast, high-resolution myocardial T_1 maps enable the detection of acute MI. Acute and chronic MI show different patterns of T_1 changes that influence DE imaging. Standardized T_1 relaxation time thresholds might be used to dichotomously identify areas of infarction, and provide a potential tool for the measurement of infarct size.

ACKNOWLEDGMENTS

This study was carried out at the British Heart Foundation (BHF) Cardiac MRI Unit, Leeds, UK. Daniel Messroghli

was supported for this work by a Marie-Curie Research Fellowship from the European Commission.

REFERENCES

1. Simonetti OP, Kim RJ, Fieno DS, Hillenbrand HB, Wu E, Bundy JM, Finn JP, Judd RM. An improved MR imaging technique for the visualization of myocardial infarction. Radiology 2001;218:215–223.
2. Kim RJ, Shah DJ, Judd RM. How we perform delayed enhancement imaging. J Cardiovasc Magn Reson 2003;5:505–514.
3. Kaldoudi E, Williams CR. Relaxation time measurements in NMR imaging. Part I: Longitudinal relaxation time. Concepts Magn Reson 1993; 5:217–242.
4. Bottomley PA, Foster TH, Argersinger RE, Pfeifer LM. A review of normal tissue hydrogen NMR relaxation times and relaxation mechanisms from 1–100 MHz: dependence on tissue type, NMR frequency, temperature, species, excision, and age. Med Physics 1984;11:425–448.
5. Messroghli DR, Radjenovic A, Kozerke S, Higgins DM, Sivananthan MU, Ridgway JP. Modified Look-Locker inversion recovery (MOLLI) for high-resolution T1 mapping of the heart. Magn Reson Med 2004;52: 141–146.
6. Messroghli DR, Plein S, Higgins DM, Walters K, Jones TR, Ridgway JP, Sivananthan MU. Human myocardium: single-breath-hold MR T1 mapping with high spatial resolution—reproducibility study. Radiology 2006;238:1004–1012.
7. Messroghli DR, Bainbridge GJ, Alfakih K, Jones TR, Plein S, Ridgway JP, Sivananthan MU. Assessment of regional left ventricular function: accuracy and reproducibility of positioning standard short-axis sections in cardiac MR imaging. Radiology 2005;235:229–236.
8. Kim RJ, Fieno DS, Parrish TB, Harris K, Chen EL, Simonetti O, Bundy J, Finn JP, Klocke FJ, Judd RM. Relationship of MRI delayed contrast enhancement to irreversible injury, infarct age, and contractile function. Circulation 1999;100:1992–2002.
9. Wagner A, Mahrholdt H, Holly TA, Elliott MD, Regenfus M, Parker M, Klocke FJ, Bonow RO, Kim RJ, Judd RM. Contrast-enhanced MRI and routine single photon emission computed tomography (SPECT) perfusion imaging for detection of subendocardial myocardial infarcts: an imaging study. Lancet 2003;361:374–379.
10. Wisenberg G, Prato FS, Carroll SE, Turner KL, Marshall T. Serial nuclear magnetic resonance imaging of acute myocardial infarction with and without reperfusion. Am Heart J 1988;115:510–518.
11. Higgins CB, Herfkens R, Lipton MJ, Sievers R, Sheldon P, Kaufman L, Crooks LE. Nuclear magnetic resonance imaging of acute myocardial infarction in dogs: alterations in magnetic relaxation times. Am J Cardiol 1983;52:184–188.
12. Abdel-Aty H, Zagrosek A, Schulz-Menger J, Taylor AJ, Messroghli D, Kumar A, Gross M, Dietz R, Friedrich MG. Delayed enhancement and T2-weighted cardiovascular magnetic resonance imaging differentiate acute from chronic myocardial infarction. Circulation 2004;109:2411–2416.
13. Flacke SJ, Fischer SE, Lorenz CH. Measurement of the gadopentetate dimeglumine partition coefficient in human myocardium in vivo: normal distribution and elevation in acute and chronic infarction. Radiology 2001;218:703–710.
14. Li G, Xiang B, Dai G, Shaw A, Liu H, Yang B, Jackson M, Deslauriers R, Tian G. Tissue edema does not change gadolinium-diethylenetriamine pentaacetic acid (Gd-DTPA)-enhanced T1 relaxation times of viable myocardium. J Magn Reson Imaging 2005;21:744–751.
15. Pereira RS, Prato FS, Sykes J, Wisenberg G. Assessment of myocardial viability using MRI during a constant infusion of Gd-DTPA: further studies at early and late periods of reperfusion. Magn Reson Med 1999;42:60–68.
16. Yan AT, Shayne A, Chan C, Reynolds HG, Tsang S, Di Carli MF, Kwong R. Characterization of peri-infarct myocardial tissue with contrast-enhanced cardiac MRI predicts post-infarction mortality beyond left ventricular ejection fraction. In: Proceedings of the 13th Annual Meeting of ISMRM, Miami Beach, FL, USA, 2006 (Abstract 44).
17. Amado LC, Gerber BL, Gupta SN, Rettmann DW, Szarf G, Schock R, Nasir K, Kraitchman DL, Lima JA. Accurate and objective infarct sizing by contrast-enhanced magnetic resonance imaging in a canine myocardial infarction model. J Am Coll Cardiol 2004;44:2383–2389.
18. Wu KC, Zerhouni EA, Judd RM, Lugo-Olivieri CH, Barouch LA, Schulman SP, Blumenthal RS, Lima JA. Prognostic significance of microvascular obstruction by magnetic resonance imaging in patients with acute myocardial infarction. Circulation 1998;97:765–772.
19. Amado LC, Kraitchman DL, Gerber BL, Castillo E, Boston RC, Grayzel J, Lima JA. Reduction of "no-reflow" phenomenon by intra-aortic balloon counterpulsation in a randomized magnetic resonance imaging experimental study. J Am Coll Cardiol 2004;43:1291–1298.
20. Maceira AM, Joshi J, Prasad SK, Moon JC, Perugini E, Harding I, Sheppard MN, Poole-Wilson PA, Hawkins PN, Pennell DJ. Cardiovascular magnetic resonance in cardiac amyloidosis. Circulation 2005;111: 186–193.
21. Mahrholdt H, Goedecke C, Wagner A, Meinhardt G, Athanasiadis A, Vogelsberg H, Fritz P, Klingel K, Kandolf R, Sechtem U. Cardiovascular magnetic resonance assessment of human myocarditis: a comparison to histology and molecular pathology. Circulation 2004;109:1250–1258.
22. Friedrich MG, Strohm O, Schulz-Menger J, Marciniak H, Luft FC, Dietz R. Contrast media-enhanced magnetic resonance imaging visualizes myocardial changes in the course of viral myocarditis. Circulation 1998;97:1802–1809.